Biomaterials Science

ROYAL SOCIETY OF CHEMISTRY

PAPER

View Article Online
View Journal | View Issue



Cite this: *Biomater. Sci.*, 2025, **13**, 3576

# Functionalization of viscoelastic gels with decellularized extracellular matrix microparticles enhances tissue adhesion, cell spreading, and tissue regeneration†

Debabrata Palai,[a] Hana Yasue,[a,b] Shima Ito,[a,c] Hiyori Komatsu,[a,c] Tetsushi Taguchi *[a,c] and Akihiro Nishiguchi *[a,b]

Received 11th March 2025,
Accepted 25th April 2025

DOI: 10.1039/d5bm00394f

rsc.li/biomaterials-science

The natural extracellular matrix (ECM) is viscoelastic and fibrous, which are crucial characteristics for controlling cellular responses. In contrast, synthetic gels are mostly elastic and less effective at promoting mechanotransduction. Thus, the design of gels that provide mechanical and biochemical cues for tissue regeneration needs to be explored. In this study, we aimed to develop viscoelastic gels functionalized with decellularized ECM (dECM) microparticles for tissue regeneration. The incorporation of dECM microparticles into gels improved not only the tissue adhesive properties of the gels but also their viscoelasticity. The modulation of the mechanical properties of the gels elicited cell adhesion and spreading. Moreover, the functionalization of viscoelastic gels with dECM microparticles promoted tissue regeneration in volumetric muscle-loss models. This approach would be a powerful method because functional scaffolds with sufficient mechanical and biological properties facilitate tissue regeneration.



## Introduction

The decellularized extracellular matrix (dECM) has emerged as a primary candidate in the fields of tissue engineering and regenerative medicine to repair and regenerate damaged tissues. The dECM is prepared by removing the cellular component and associated antigens from native tissue, while concurrently preserving its structural integrity and non-cellular components.[1] The dECM comprises a variety of proteins and glycosaminoglycans, providing a fibrous network platform to mediate mechanical and biochemical signaling between cells, which can improve cellular function and promote tissue repair and remodelling.[2–6] However, dECM scaffolds, including sheets and fibers, have drawbacks in their practical use because of their lack of injectability and tissue-adhesive properties, which limit their clinical translation. Although solubilized dECM can form gels post-injection, enzymatic treatment impairs its mechanical and viscoelastic properties.[7,8]

To overcome these challenges, the dECM can be combined with hydrogels. Hydrogels are promising biomaterials for tissue regeneration because of their biocompatibility, biodegradability, and tunable mechanical and biological functionalities.[9–11] Aside from tissue regeneration, hydrogels have been used in various other biomedical applications, such as tissue scaffold adhesives[12–14] for *in vitro* vascularization[15] and anti-inflammatory drug carriers.[16,17] However, covalently crosslinked synthetic hydrogels are mostly elastic and prevent many cellular functions observed in the natural ECM.[18,19] The natural ECM is viscoelastic and possesses complex structures because of the distinct structural arrangement of various biopolymers. With these features, the ECM regulates cellular functions, such as spreading, migration, proliferation, and differentiation.[20,21] Hence, to design tissue regenerative materials, viscoelastic scaffolds with mechanical and biochemical properties similar to those of the natural ECM need to be developed.[22–24] Recent research has focused on dECM fibers or particles, which are subsequently reconstituted into various biomaterial forms, such as hydrogels and electrospun scaffolds.[25,26] Decellularized extracellular matrix (dECM)-based hydrogels have been widely reported as promising materials for tissue regeneration. However, the design and optimization of viscoelastic gels modified with dECM microparticles remain largely unexplored, presenting an opportunity for further investigation in biomaterial engineering.

[a]*Biomaterials Field, Research Center for Macromolecules and Biomaterials, National Institute for Materials Science, 1-1 Namiki, Tsukuba, Ibaraki 305-0044, Japan. E-mail: nishiguchi.akihiro@nims.go.jp, taguchi.tetsushi@nims.go.jp*
[b]*Department of Materials Science and Technology, Graduate School of Advanced Engineering, Tokyo University of Science, 6-3-1 Niijuku, Katsushika-ku, Tokyo 125-8585, Japan*
[c]*Graduate School of Pure and Applied Sciences, University of Tsukuba, 1 Chome-1-1 Tennodai, Tsukuba, Ibaraki 305-8577, Japan*

†Electronic supplementary information (ESI) available: Supplementary Fig. S1 and S2. See DOI: https://doi.org/10.1039/d5bm00394f

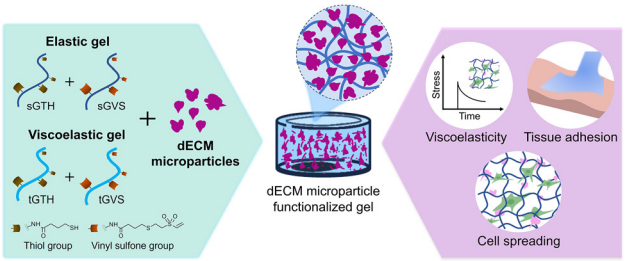


**Fig. 1** Schematic of the preparation of dECM microparticle-functionalized elastic and viscoelastic gels crosslinked *via* the thiol–ene reaction. Two types of gelatin from different sources were chemically modified with thiol (TH) and vinyl sulfone (VS) groups: porcine skin-derived gelatin (sG) with TH (sGTH) and VS (sGVS) and porcine tendon-derived gelatin (tG) with TH (tGTH) and VS (tGVS). The incorporation of decellularized extracellular matrix (dECM) microparticles can alter gel properties, including stress relaxation, tissue adhesion, cell–material interaction and tissue repair.

In this study, we developed viscoelastic gels functionalized with dECM microparticles for tissue regeneration (Fig. 1). Gelatin from two different sources (porcine-skin-derived gelatin [sG] and porcine tendon-derived gelatin [tG]) was chemically modified with thiol and vinyl sulfone groups and crosslinked to form elastic and viscoelastic gels, respectively. We addressed the effect of incorporating dECM microparticles into gels on mechanical properties, such as stress relaxation and tissue adhesiveness. The effects of these properties on cellular behavior and function were thoroughly investigated. Moreover, the treatment of a defect in muscle tissue, volumetric muscle loss (VML), using dECM microparticle-functionalized gels was demonstrated to evaluate the tissue-regenerative properties.

# Experimental

## Materials

Porcine-skin-derived gelatin (sG, $M_w$ = 180 kDa) and porcine-tendon-derived gelatin (tG, $M_w$ = 344 kDa) were purchased from Nitta Gelatin, Inc. (Osaka, Japan). 2,4,6-Trinitrobenzenesulfonic acid sodium salt dihydrate (TNBS) was purchased from Tokyo Chemical Industry Co. Ltd (Tokyo, Japan). Tris(2-carboxyethyl) phosphine hydrochloride (TCEP) and phosphate-buffered saline (PBS) were purchased from Nacalai Tesque, Inc. (Kyoto, Japan). 5,5′-(2-Nitrobenzoic acid) (DTNB), RPMI 1640 medium, and fetal bovine serum (FBS) were purchased from Sigma-Aldrich (St Louis, MO, USA). Collagen casings were purchased from Nippi (Tokyo, Japan). Penicillin/streptomycin (P/S), trypsin, rhodamine-labelled phalloidin, and 4′,6-diamidino-2-phenyl-indole (DAPI) were purchased from Thermo Fisher Scientific (Waltham, MA, USA). Amikacin solution was purchased from Meiji Seika Pharma (Tokyo, Japan). Dialysis membranes (molecular weight cut-off value: 12 000–14 000) were purchased from Repligen (Waltham, MA, USA). DNase I was purchased from Merck (Darmstadt, Germany). Dimethyl sulfoxide (DMSO), peracetic acid (PA), magnesium sulfate, and proteinase K were purchased from Fujifilm (Osaka, Japan). The mouse myoblast cell line (C2C12 cells) was purchased from the European Collection of Authenticated Cell Cultures (Salisbury, UK).

## Preparation of dECM microparticles

Decellularization of tissues from the urinary bladder was performed as described in a previous report.[27] Briefly, a purchased porcine urinary bladder (Tokyo Shibaura Zouki, Tokyo, Japan) was cut open, and the mucosal layer was dissected using a scalpel. The mucosa was washed with saline and incubated in PBS containing 0.1% PA and 4% ethanol for 2 h at 25 °C. The tissues were then washed twice with 1 L of saline and 1 L of ultrapure water for 1 h each at 25 °C and freeze-dried. The dried tissues were cut into small pieces using scissors and 10 mg of tissue fragments were incubated in 1 mL of PBS containing DNase I (0.2 mg $mL^{-1}$, 300 U $mL^{-1}$; Roche Diagnostics, Indianapolis, IN, USA) and 5 mM magnesium sulfate at 37 °C for 24 h with stirring. The samples were collected by centrifugation at 10 000 rpm for 10 min and washed twice with 2 mL of PBS and 2 mL of ultrapure water for 10 min at 25 °C, respectively. After repeating the washing and freeze-drying steps, the urinary bladder matrix (UBM)-based dECM was obtained.

dECM microparticle fabrication was performed according to a previous report, with slight modifications.[28] Freeze-dried dECM sheets were cut into small pieces and ground using a grinder (Wonder Crusher; Osaka Chemical, Osaka, Japan). The ground dECM was further cryo-milled using a cryogenic grinder machine (6775 FREEZER/MILL; SPEX, USA), loaded into small grinding vials, precooled for 1 min under liquid nitrogen, and cryo-milled for two cycles at 15 cycles per second for 2 min, followed by 2 min of rest for a total of 7 min each. The morphology of the dECM microparticles was observed using scanning electron microscopy (SEM) (JCM-7000 NeoScope; JEOL, Tokyo, Japan). The dECM microparticles were attached to a carbon tape, and sputtered with gold for 1 min. To obtain the SEM images of the particles, the accelerating voltage and working distance were set to 15 kV and 12.7 mm, respectively. The size distribution of the dECM microparticles was analyzed using ImageJ software (National Institutes of Health, Bethesda, MD, USA).

## Quantification of DNA content

The DNA content of the tissues before and after the decellularization process was quantified according to a previous report.[27] Briefly, the dried dECM (10 mg) was dispersed in 1 mL of proteinase K (50 μg $mL^{-1}$) in a mixture of 10 mM Tris-HCl buffer, 10 mM ethylenediaminetetraacetic acid (EDTA), 10 mM NaCl, and 0.5% sodium dodecyl sulfate (pH = 8) and incubated at 37 °C for 24 h. The solution was then mixed with 500 μL of a phenol/chloroform/isoamyl alcohol (25/24/1) solution and centrifuged at 15 000 rpm at 4 °C for 30 min. After collecting the aqueous layer, 50 μL of acetic acid solution (3 M) was added (final concentration: 300 mM). DNA was precipi-

tated by the addition of a two-fold excess (1 mL) of cold ethanol and stored at −20 °C for 1 h. After centrifuging the solution at 15 000 rpm for 30 min, the supernatant was removed, and the precipitate was dried under vacuum for 30 min. The samples were resuspended in 1 mL of Tris-HCl buffer (10 mM) with EDTA (1 mM) and diluted 10-fold. The remaining DNA content was measured using a PicoGreen™ dsDNA Assay Kit (Thermo Fisher Scientific) according to the manufacturer's instructions. Sample fluorescence was recorded using a microplate reader (Spark10M; TECAN, Mannedorf, Switzerland). The DNA content was calculated using a standard curve.

### Synthesis of sGTH, tGTH, sGVS, and tGVS

To synthesize gelatin modified with thiol groups, 1 g of sG (amino groups: 292 μmol $g^{-1}$) and tG (263 μmol $g^{-1}$) was dissolved in 13.6 mL and 22 mL of DMSO, respectively, and stirred at 50 °C for 4 h. The number of amino groups in the gelatin samples was determined using the TNBS method. γ-Thiobutyrolactone (60.5 μL, 240 mol% equivalent to the amino groups in sG, and 50 μL, 220 mol% equivalent to the amino groups in tG) was dissolved in 3 mL of DMSO and added to the solution. The reaction was continued overnight at 50 °C with stirring. To reduce the disulfide bonds to thiol groups, TCEP (1 mM) was added, and the mixture was stirred for 30 min at room temperature. The resulting solutions were slowly added to a 20 vol% cold solvent mixture (ethanol and ethyl acetate, v/v = 1/1) while stirring, and the precipitates were collected using a glass filter and washed three times with ethanol to remove unreacted reagents. The precipitates collected by filtration were dried at room temperature under reduced pressure for 3 days to obtain sGTH and tGTH. The degree of substitution of the thiol groups was calculated using the Ellman method, as reported elsewhere.[12]

To synthesize gelatin modified with vinyl sulfone (sGVS and tGVS), 1 g of sGTH or tGTH was dissolved in 99 mL of ultrapure water at 50 °C with stirring for 1 h. Divinyl sulfone (200 and 120 mol% equivalent to the thiol groups in sGTH and tGTH, respectively) was dissolved in 1 mL of ultrapure water and added dropwise to the solution. The reaction was continued for 24 h at 50 °C with continuous stirring. TCEP (1 mM) was added to the solution, and the obtained solution was dialyzed in ultrapure water using a dialysis membrane for 3 days. After freeze-drying, sGVS and tGVS were obtained.

### Evaluation of tissue-adhesive properties

The tissue-adhesive properties of the gels were evaluated by measuring the burst strength according to the American Society of Testing and Materials (ASTM) procedure (ASTM-F2392-04R, standard test method for burst strength of surgical sealants). Collagen casings (Nippi) were cut into 35 mm discs with 3 mm pinholes at the center. A silicone ring mold (outer and inner diameters: 20 and 10 mm, respectively; thickness: 1 mm) was placed on the collagen casings. sGTH, sGVS, tGTH, and tGVS were dissolved in PBS (10 wt%) at 50 °C with stirring and the pH was adjusted to 7.4, 6.4, 7.4, and 6.4, respectively, using 1 M NaOH. The solution was maintained at 37 °C until further use. Solutions of sGTH (200 μL) and sGVS (200 μL) or tGTH (200 μL) and tGVS (200 μL) were vigorously mixed using a pipette. The dECM microparticles (40 mg, final concentration: 10 wt%) were mixed using a spatula. Three hundred microliters of the mixed solution was placed onto the collagen casings inside the silicon mold ring. After 60 min of gelation at 37 °C, the silicone mold was removed, and the samples were placed in the chamber. Burst strength (maximum pressure until rupture) was measured by running saline water using a syringe pump at a flow rate of 2 mL $min^{-1}$ at 37 °C.

### Rheological analysis

Rheological measurements were performed using a rheometer (MCR301; Anton Paar GmbH, Graz, Austria). sGTH–sGVS or tGTH–tGVS gels, with or without dECM microparticles (10 wt%), were prepared to evaluate gelation kinetics and viscoelastic properties. The pre-gel solution was placed on the stage of the rheometer (pre-heated at 37 °C) and a jig with a 10 mm diameter was set up with a gap of 1 mm. After removing the excess gel, measurements were performed at 37 °C at a frequency of 10 rad $s^{-1}$ with 1% strain for 1 h. The stress relaxation properties of the gels and dECM-modified gels were measured at 0.2% strain with a deformation rate of 1 mm $min^{-1}$.

### Cell encapsulation

sGTH, tGTH, sGVS, and tGVS were dissolved in PBS (10 wt%) at 50 °C with stirring and the pH was adjusted to 7.4 and 6.4, respectively, with 1 M NaOH. All solutions were filtered using a 0.45 μm syringe filter for sterilization. The solutions were stored at 37 °C until further use. C2C12 cells were cultured in RPMI medium supplemented with 10% FBS and 1% P/S. Cultured cells were treated with trypsin and the cell pellet was collected after centrifugation at 1200 rpm for 5 min at 4 °C. After removing the supernatant, 200 μL of sGTH–sGVS or tGTH–tGVS mixtures, with or without 10 wt% dECM microparticles, were added to each tube containing the cell pellet ($1 \times 10^5$ cells) as distinct groups. Twenty microliters of pre-gel samples containing cells were plated on a chamber cover (10 × 10 mm). The samples were then incubated for 10 min at 37 °C for gelation. Four hundred microliters of RPMI medium with 10% FBS and 1% P/S was then added to each chamber and the cells were cultured for 1 d at 37 °C in a 5% $CO_2$ incubator.

### Fluorescence staining, imaging, and analysis

Cells encapsulated in gels were fixed with 4% paraformaldehyde for 1 h. After washing with PBS, the cells were permeabilized with 0.2% Triton-X for 30 min. After washing the sample with PBS, the cells were blocked with 1% bovine serum albumin/PBS for 1 h. For actin staining, the cells were stained with rhodamine-labelled phalloidin (1 : 100) overnight at 25 °C. After washing with PBS, the cells were stained with DAPI for 1 h at 25 °C. The cell morphology was observed at a depth of 50 μM using confocal laser scanning microscopy

 

(CLSM; CLSM 900 with Airyscan2; Zeiss, Oberkochen, Germany) and the area of the cells and the average length of elongated cells were quantified in at least three different images using ImageJ. Correlation studies were conducted between the average cell length and half relaxation time ($t_{1/2}$) using Python 3.10.12 run in Google Colaboratory (Colab) to clarify the relationship between the two metrics.

### Biodegradability test

All animal procedures were performed in accordance with the Guidelines for Care and Use of Laboratory Animals of National Institute for Materials Science and approved by the Animal Ethics Committee of the National Institute for Materials Science (no: 76-2023-16). To maintain uniformity in the size of the gels, pre-crosslinked gels were used for biodegradability testing. Two milliliters of tGTH-tGVS pre-gel solution with or without dECM microparticles (10 wt%) were placed on a 1 mm-thick silicone mold, followed by incubation for 1 h at 37 °C. The crosslinked gels were then cut into disc shapes using an 8 mm biopsy punch (KAI Medical, Seki City, Japan). Mice (7 week-old female C57BL/6J mice; Jackson Laboratory, Bar Harbor, ME, USA) were anesthetized *via* inhalation of 2% isoflurane. The backs of the mice were disinfected with 70% ethanol and the hair was trimmed. Gel discs (1 mm thick) were subcutaneously implanted in each mouse on the left and right sides of the dorsal region. At 3, 7, 14, and 28 days after implantation, the mice were euthanized by exsanguination, and tissues were collected. For sham, subcutaneous tissues without implantation of gels were collected. The obtained tissues were fixed in 10% formalin buffer solution for 3 days, embedded in paraffin, sectioned, and stained with hematoxylin and eosin (HE). Tissue images were scanned using a digital slide scanner (NanoZoomer S210; Hamamatsu Photonics, Hamamatsu, Japan).

### VML model

Volumetric muscle recovery using dECM microparticle-functionalized viscoelastic gels was investigated. Mice (7 week-old female C57BL/6J mice, Jackson Laboratory) were anesthetized *via* inhalation of 2% isoflurane. The hair on the hindlimb of the mice was trimmed and disinfected using 70% ethanol. An incision was made to expose the tibialis anterior (TA) muscle and a defect ($5 \times 2 \times 2$ mm$^3$) was created. The viscoelastic gels with dECM microparticles were mixed using a spatula and approximately 10 μL was transferred carefully to the defect site. The skin wounds were sutured for closure, and all mice were intraperitoneally administered amikacin (1 mg kg$^{-1}$). After 28 days, the mice were euthanized by exsanguination and muscle tissues were collected. The obtained tissues were weighed and fixed in 10% formalin buffer for 3 days, embedded in paraffin, sectioned, and stained with HE and Masson's trichrome (MT). The tissue images were scanned using a digital slide scanner. Muscle area was quantified from cross-sectional HE-stained images using ImageJ and the area of the control sample was set as 100%.

### Statistical analysis

The results are expressed as the mean ± standard deviation. One-way analysis of variance (ANOVA) followed by Tukey's multiple comparisons *post-hoc* test was used to assess differences among groups. Experiments were repeated multiple times on independent occasions. The data shown in each figure are complete datasets from representative independent experiments. None of the samples were excluded from the analysis. Statistical significance is indicated as $^{*}P < 0.05$, $^{**}P < 0.01$, $^{***}P < 0.001$, and $^{****}P < 0.0001$. Statistical analyses were performed using GraphPad Prism software (version 8.0; GraphPad Software, San Diego, CA, USA). Pearson's correlation analysis was performed using Google Colab and Python version 3.10.12.

## Results and discussion

### Stress relaxation property in gels with dECM microparticles

Living tissues and organisms microscopically appear to be solid or elastic, but they are not exactly so.[29] They exhibit time-dependent mechanical responses or dissipate partially the energy applied to deform them. This is known as viscoelastic behaviour.[30] The viscoelasticity of natural tissues is regulated by the temporal and spatial arrangement of the surrounding ECM, which regulates cell behaviors in favor of tissue regeneration.[24,29] Therefore, artificial scaffolds designed for tissue regeneration need to possess appropriate mechanical characteristics, especially viscoelastic behavior, together with the necessary biochemical properties. To develop tissue-regenerative scaffolds, the dECM was incorporated into gels. The dECM was prepared by the decellularization and cryo-milling of UBM samples (Fig. 2a). UBM, consisting of the lamina propria and basal lamina, has been suggested to provide a pro-regenerative microenvironment in injured tissues because of its inherent immunomodulatory properties, such as the recruitment of immune cells and macrophage polarization.[31] After the decellularization process of the urinary bladder using PA and DNase treatment, the DNA content decreased from 2126 ng mg$^{-1}$ in the native tissue to 20 ng mg$^{-1}$ in the dECM (Fig. 2b). This result satisfied the minimal criterion of a remaining DNA level of <50 ng mg$^{-1}$.[36] SEM observations showed that the cryo-milled dECM consisted of micrometer-sized fragments with different diameters, which we termed dECM microparticles (Fig. 2c). The results of particle size analysis revealed that the average particle diameter was 9 μm (Fig. 2d).

To prepare the gels, two types of gelatin derived from different sources, skin and tendon (sG and tG), were used as the main polymers. sG and tG gelatins were chemically modified with thiol and vinyl sulfone groups to obtain sGTH, tGTH, sGVS, and tGVS, respectively. The introduction of the thiol and vinyl sulfone groups was confirmed using the TNBS method (Table 1). The sGTH, sGVS, and tGTH, tGVS solutions were mixed (v/v = 1 : 1) at 37 °C to prepare sGTH–sGVS or tGTH–tGVS gels *via* a Michael addition reaction. To prepare dECM-

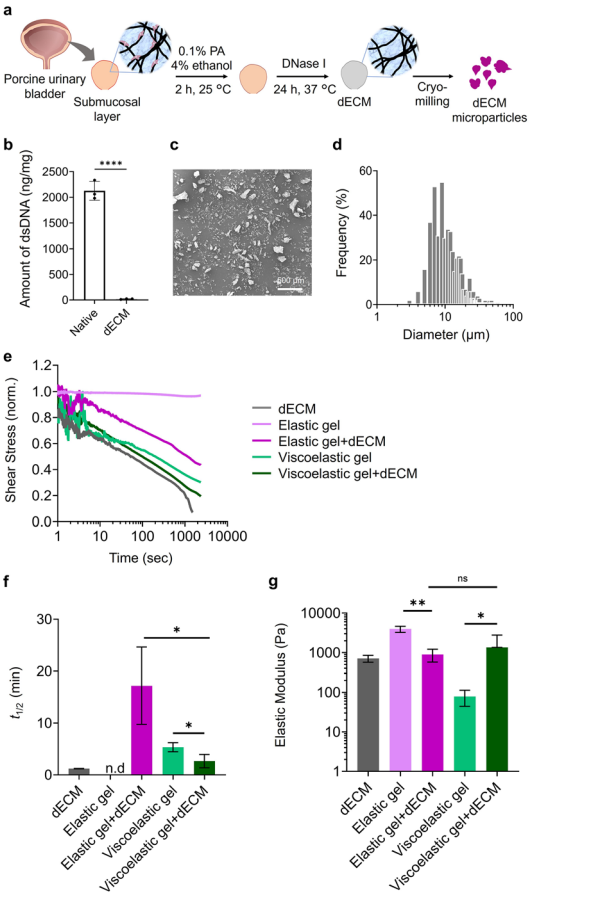


**Fig. 2** (a) Schematic illustration of the decellularization process of submucosal tissues obtained from the porcine urinary bladder to prepare dECM microparticles. (b) DNA content of native tissue and dECM ($n$ = 3). (c) Scanning electron microscopy images of dECM microparticles. (d) Distribution of dECM microparticles with different diameter sizes. (e) Rheological measurements of the stress relaxation of gels and dECM-modified gels at 20% strain. The sGTH–sGVS gel and tGTH–tGVS gel were referred to as the elastic gel and viscoelastic gel, respectively. (f) Quantification of the timescale at which the stress is relaxed to half of its original value, $t_{1/2}$, from the stress relaxation tests in (e) ($n$ = 3). (g) Measurements of the elastic modulus of the gels ($n$ = 3). Data are presented as mean ± standard deviation (SD). *$P$ < 0.05, **$P$ < 0.01, and ****$P$ < 0.0001, analyzed using a two-tailed Student's $t$-test and one-way analysis of variance (ANOVA), followed by Tukey's multiple comparisons *post hoc* test. n.d. and n.s. denote not determined and not significant.

modified gels, dECM microparticles (10 wt%) were mixed with the gels at 37 °C using a spatula. Rheological measurements revealed that the tGTH–tGVS gels possessed viscoelastic properties with rapid stress relaxation, whereas the sGTH-sGVS gels were elastic with minimal stress relaxation (Fig. 2e). Previously, we reported that tG possessed a higher sol–gel transition temperature and stronger non-covalent intermolecular interactions (*e.g.*, hydrogen bonding) compared to sG, partly because sG and tG differ in their molecular structures, including their molecular weight (191 kDa for sG and 344 kDa for tG) and amino acid compositions.[30] Since it has been reported that hydrogels made of high-molecular-weight polymers show faster stress relaxation compared to those made from low-molecular-weight polymers,[32] gels composed of higher-molecular-weight tG may display rearrangement of their network structures under force, showing viscoelastic behaviors. Based on these results, we refer to sGTH–sGVS gels as "elastic gels" and tGTH–tGVS gels as "viscoelastic gels".

Next, we investigated the effect of incorporating dECM microparticles into the gels on their rheological properties. Time-dependent rheological evaluation revealed that the elastic modulus of each gel reached a plateau within 1 h, indicating the completion of gel formation (ESI Fig. S1†). The incorporation of the dECM microparticles also increased gelation speed. Importantly, the incorporation of dECM microparticles into the gels modulated the viscoelastic properties of the gels, resulting in faster stress relaxation under a fixed strain of 20% for both gels. The half relaxation time ($t_{1/2}$) of the viscoelastic gels decreased from 5.3 min to 2.6 min and the relaxation time for the elastic gels changed from undefined to 17 min, indicating that the incorporation of the dECM significantly accelerated the rate of stress relaxation in the gels (Fig. 2f). Previous studies have reported that incorporating collagen into gels can improve the stress relaxation rate.[10] The incorporated dECM microparticles may function as fillers in the gels and dissipate energy under stress by rearranging their structures. The incorporation of dECM microparticles into the elastic and viscoelastic gels affected their elastic moduli differently, but the dECM microparticle-incorporated elastic and viscoelastic gels possessed almost the same elastic modulus (Fig. 2g).

### Enhanced tissue adhesiveness by dECM microparticles

The tissue adhesion of gels to defects is essential for closing wounds and avoiding the leakage of body fluids or blood. It

**Table 1** Synthesis of thiolated and vinyl sulfonated gelatin with different degrees of substitution

| | γ-Thiobutyrolactone (equivalent to amino group in gelatin) | Divinyl sulfone (mol% to thiol) | Amount of TH (μmol $g^{-1}$) | Amount of VS (μmol $g^{-1}$) | DS (%) | Yield (%) |
|---|---|---|---|---|---|---|
| sGTH | 240 | — | 232 | — | 40 | 88 |
| sGVS | — | 200 | 1 | 231 | 79 | 85 |
| tGTH | 220 | — | 130 | — | 50 | 90 |
| tGVS | — | 120 | 9 | 121 | 36 | 91 |

TH, thiol; VS, vinyl sulfone; DS, degree of substitution; sG, skin-derived gelatin; and tG, tendon-derived gelatin.

contributes to the promotion of tissue regeneration and the prevention of postoperative complications. The burst strengths of the gels were evaluated using an adhesion test setup with a collagen casing (Fig. 3a). The dECM microparticle-functionalized gels remained intact in the defect of the collagen casing for a long period of time and revealed a much higher burst pressure than the gels without the dECM (Fig. 3b and c). dECM paste without gels often shows low mechanical strength, poor stability, and rapid degradation, which was also evident in this study, where the dECM possessed a burst strength of 0.4 kPa. In contrast, the incorporation of dECM microparticles into gels significantly improved the bulk strength of the gels and the burst strength because of the combination of chemical bonding between the thiol–ene reaction and the physical interaction between collagen fibers present in the dECM microparticles. Furthermore, chemical anchoring with functional groups in collagen casings may support interfacial adhesion to improve the adhesion strength to tissues.[31,32] The burst strength increased 2.4-fold in an elastic gel and 2-fold in a viscoelastic gel after incorporating the dECM microparticles by increasing the cohesive strength of gels through physical interactions between the polymer and microparticles. When dECM powder that was not cryo-milled was incorporated with gels, the burst strength reduced by almost half compared to that with dECM microparticles, indicating that the size of the dECM has a great impact on the cohesive strength of gels (ESI Fig. S2†). The elastic gel exhibited more improvement in strength because of the presence of a large number of thiol and vinyl sulfone groups compared to the viscoelastic gels. Viscoelastic hydrogels may have lower burst strength compared to purely elastic gels, due to their ability to dissipate energy through viscous flow rather than maintaining structural integrity under sudden stress. Such differences in strength are also reported in previous studies.[33,34]

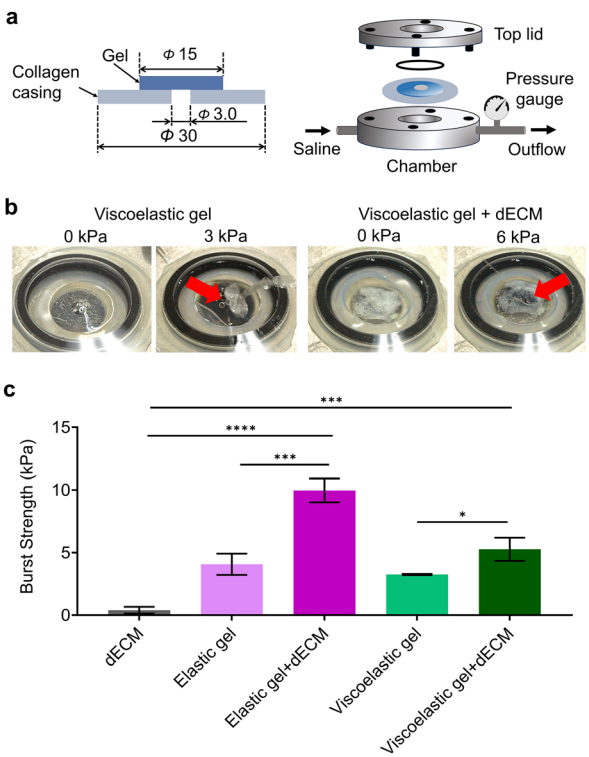


**Fig. 3** Tissue-adhesive properties of gels. (a) Setup for the measurement of burst strength. (b) Macroscopic images of burst pressure measurements. (c) Burst strength of the dECM and elastic gels and viscoelastic gels with dECM microparticles ($n$ = 3). Data are presented as the mean ± SD. *$P$ < 0.05, ***$P$ < 0.001, and ****$P$ < 0.0001, analyzed using one-way ANOVA, followed by Tukey's multiple comparisons *post hoc* test.

### Effect of stress relaxation on cell spreading

For tissue remodeling and regeneration, it is crucial to design gel scaffolds with tunable viscoelasticity and profound mechanical strength.[35,36] Cell encapsulation tests were performed to address the influence of stress relaxation and biochemical cues in gels on cellular behavior. Mouse myoblasts (C2C12 cells) were encapsulated and cultured in elastic and viscoelastic gels, with and without dECM microparticles. The CLSM observations revealed that cell adhesion and spreading were suppressed in the elastic gel, which required a longer time to relax the applied stress (Fig. 4a). Although the dECM microparticle functionalization of elastic gels improved the timescale for stress relaxation of elastic gels ($t_{1/2}$ ~18 min), the morphology of most of the cells remained round. In contrast, the cell adhesion area and length of the adhered cells significantly increased in viscoelastic gels with dECM microparticles with faster stress relaxation ($t_{1/2}$–3 min) compared to gels without the dECM (Fig. 4b and c). Cell proliferation was confirmed over time in a viscoelastic gel containing the dECM (ESI Fig. S3†). This indicated that C2C12 cell adhesion and spreading were influenced by the viscoelasticity of the matrix. Notably, the incorporation of dECM microparticles into viscoelastic gels significantly improved cell spreading compared to that of viscoelastic gels alone, indicating that both mechanical (enhanced stress relaxation) and biological (cell-adhesive ligands on the dECM) cues may be associated with cell behavior. Although bioactive molecules in dECM-incorporated gels influenced cell adhesion, the length of the elongated cell had a moderate negative correlation (correlation co-efficient: −0.31) with $t_{1/2}$, suggesting that the faster stress relaxation of the matrix likely supports cell adhesion and spreading (Fig. 4d). Many previous studies have highlighted the importance of gel matrix remodeling on cell functions.[10,29,35] Cells initially employ strain on the gel matrix, and depending on the elastic modulus, the matrix resists strain and prevents deformation. In this study, the elastic gel showed no relaxation of the applied forces or a prolonged time. When the matrix structure is chemically crosslinked, cells are unable to spread through matrix remodeling, which results in the suppression of cellular activity.[37] Conversely, in viscoelastic gels composed of tGTH and tGVS, the forces can relax over time through physical interactions between tG. In addition, the inclusion of dECM microparticles introduced weak physical interactions between the

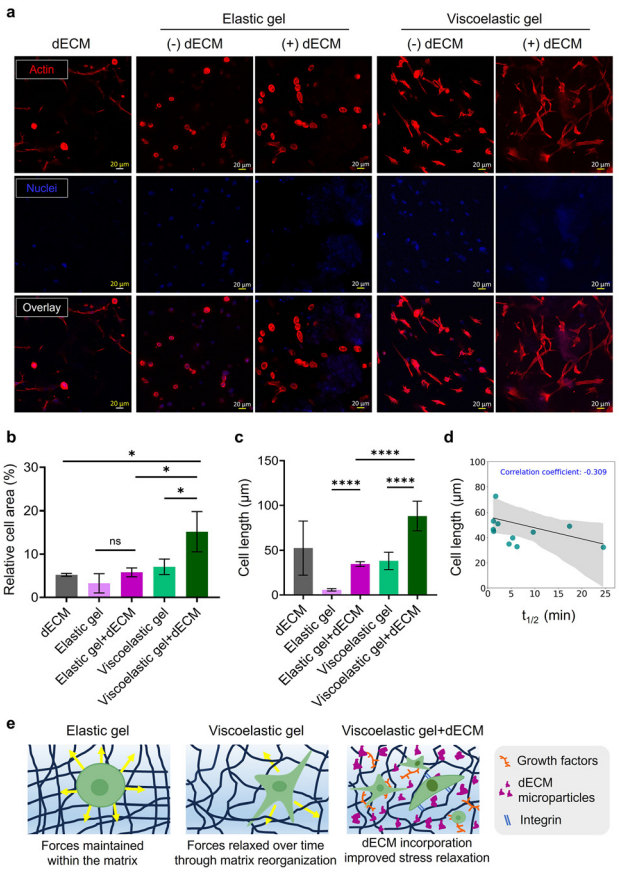


**Fig. 4** (a) Confocal laser-scanning microscopy images of cells encapsulated in elastic and viscoelastic gels with dECM microparticles for 24 h. Representative immunofluorescence staining for actin (red) and nuclei (blue). (b) Area of adherent cells in gels ($n$ = 3). (c) Average length of cells in the respective gel groups ($n$ = 5). (d) Pearson's correlation analysis between the length of the cells and the $t_{1/2}$ of each sample group. (e) Illustrations depicting the possible mechanism whereby the elasticity and stress relaxation of the matrix regulated cellular behaviors. Data are presented as the mean ± SD. *$P$ < 0.05 and **** $P$ < 0.0001 analyzed using one-way ANOVA, followed by Tukey's multiple comparison *post hoc* test. n.s. denotes not significant.

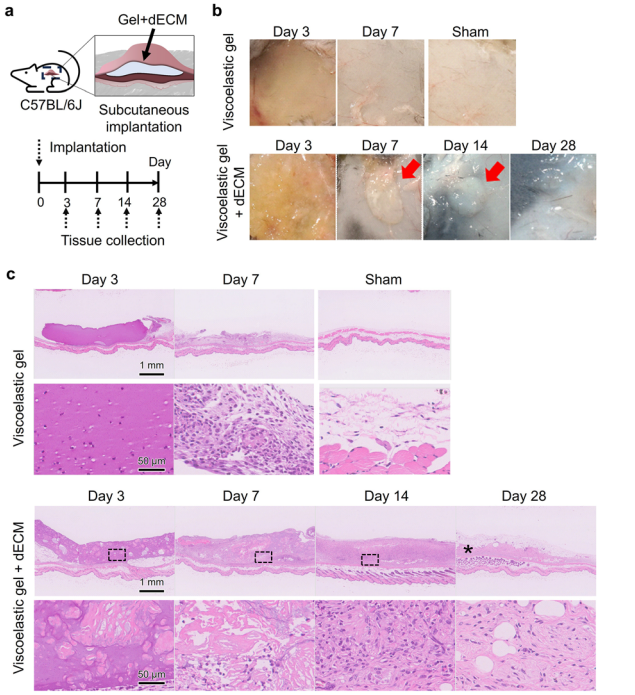


**Fig. 5** Evaluation of the biodegradability of the gels with dECM microparticles after subcutaneous implantation in mice. (a) Schematic depicting the implantation of viscoelastic gels, with and without dECM, into the subcutaneous space of mice. (b) Images of the tissues and viscoelastic gels, with and without the dECM embedded, in tissues at days 3, 7, 14, and 28. (c) Histological observation of hematoxylin and eosin–stained images of viscoelastic gels with and without dECM microparticles. The asterisk represents remaining gels or their fragments. Scale bars represent 250 μm (top) and 50 μm (bottom).

collagen fibers. This contributed to faster stress relaxation and improved cell adhesion and spreading (Fig. 4e).

### Host tissue response to viscoelastic gels with dECM microparticles

From the *in vitro* analysis, it was determined that the cells largely adhered to the dECM microparticle-functionalized viscoelastic gels by exerting strain and remodeling the gel matrix. To evaluate the host tissue response and cell–matrix interaction *in vivo*, a biodegradability test of viscoelastic gels with and without dECM microparticles was conducted by subcutaneous implantation into the dorsal region of mice (Fig. 5a). Irritation and local reaction were not observed at the implant sites in any group during the course of the study. For implantable biomaterial applications, scaffolds must have robust mechanical properties and degrade at a rate that matches the rate of new tissue ingrowth. Macroscopic images showed that the viscoelastic gels swelled on day three and degraded completely on day seven after implantation (Fig. 5b). In contrast, the viscoelastic gels with dECM microparticles showed longer structural stability and were almost completely degraded after 28 days. Histological observations of the HE-stained tissues revealed that immune cells infiltrated the viscoelastic gels within 3 days, and the gel structures degraded on day 7 (Fig. 5c). In viscoelastic gels containing dECM microparticles, immune cells accumulated on the gel surface and infiltrated the gel over time. The dECM-functionalized gels have suitable biocompatibility and rates of cell infiltration and might be useful as scaffolds for regenerative applications, such as muscle tissue regeneration.

### Tissue regeneration in VML models

Finally, we evaluated the therapeutic efficacy of the engineered gels against VML. VML is a traumatic or surgical injury to the skeletal muscles. Irrecoverable muscle tissue loss often results in chronic functional deficits and long-term disability. Although the dECM is a potent therapeutic biomaterial against VML for structurally and functionally reconstructing muscle tissues,[35] the suspension of the dECM may detach from implantation sites due to poor structural integrity and tissue

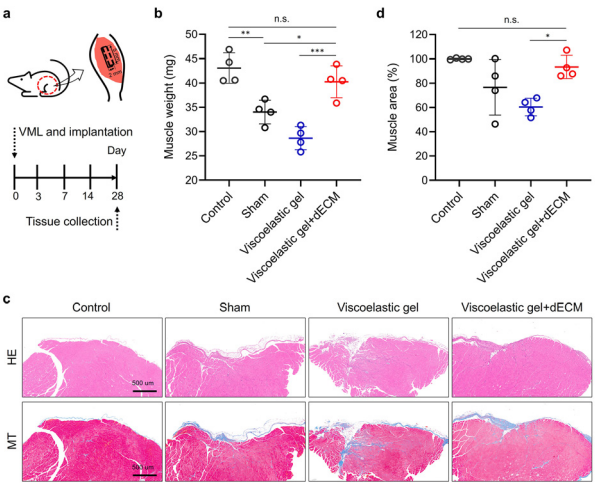


**Fig. 6** Treatment of VML using viscoelastic gels. (a) The procedure for inducing VML and the implantation of the gels. (b) Muscle weight at 28 days after VML treatment and gel implantation ($n$ = 4). (c) HE and MT stained images of VML-treated muscle tissues. (d) Area of the whole muscle tissues in HE images ($n$ = 4). Data are presented as the mean ± SD. $*P < 0.05$, $**P < 0.01$, and $***P < 0.001$, analyzed using one-way ANOVA, followed by Tukey's multiple comparisons *post hoc* test. n.s. denotes not significant.

adhesive properties under physiological conditions. Thus, tissue- and cell-adhesive gels have the potential to improve therapeutic efficacy against VML. VML defects (5 mm × 2 mm × 2 mm) were created in the TA muscle of the mice, and the gels were implanted for tissue regeneration (Fig. 6a). Twenty-eight days after VML treatment and gel implantation, muscle weight recovered in tissues treated using viscoelastic gels with dECM microparticles compared to tissues treated with sham and viscoelastic gels without the dECM (Fig. 6b). Histological observations of HE-stained tissue sections revealed that viscoelastic gels with dECM microparticles increased the area of muscle tissues compared to viscoelastic gels alone (Fig. 6c and d). Moreover, Masson's trichrome staining showed that the fibrotic area did not increase in muscle tissues treated with viscoelastic gels with dECM microparticles compared to the control. These results indicated that engineered gels with viscoelastic, tissue-adhesive, and cell-adhesive properties can promote muscle tissue regeneration in VML models. In addition to the mechanical features (viscoelasticity and tissue adhesiveness) provided by dECM microparticles, the biochemical features of the dECM, including the presentation of cell-adhesive ligands, the secretion of biological signals, and the interaction with immune cells, may affect therapeutic efficacy.

## Conclusions

In conclusion, this study presents the engineering of a viscoelastic, biocompatible, and tissue-adhesive dECM-based gel scaffold. Thiol–ene crosslinking improved mechanical strength and tissue adhesion, whereas dECM microparticles provided the necessary biological cues for cell adhesion and tissue modeling. The gelation speed and mechanical properties of the viscoelastic gel were also improved by incorporating dECM microparticles. The dECM-based gels had a faster rate of stress relaxation than the gels themselves, which led to enhanced cell adhesion and spreading. The dECM-modified gels showed high biocompatibility when implanted subcutaneously in mice. Thus, dECM-incorporated viscoelastic gels can provide tissue regenerative properties through biological interactions with tissues. This dECM-based viscoelastic gel can be used as a biofunctional and tissue-adhesive scaffold to promote tissue remodeling and regeneration.

## Data availability

Data generated during the study are available from the corresponding author upon request.

## Conflicts of interest

There are no conflicts to declare.

## Acknowledgements

We acknowledge the financial support from the Japan Society for the Promotion of Science (JSPS) KAKENHI (grant no. 22H03962, 23H01718, 23K26411, and 24K21677) and the Uehara Memorial Foundation.

## References

1 M. T. Wolf, *Adv. Drug Delivery Rev.*, 2015, **84**, 208–221.
2 M. P. Lutolf and J. A. Hubbell, *Nat. Biotechnol.*, 2005, **23**, 47–55.
3 D. O. Freytes, J. Martin, S. S. Velankar, A. S. Lee and S. F. Badylak, *Biomaterials*, 2008, **29**, 1630–1637.
4 E. Vorotnikova, *Matrix Biol.*, 2010, **29**, 690–700.
5 B. N. Brown, J. E. Valentin, A. M. Stewart-Akers, G. P. McCabe and S. F. Badylak, *Biomaterials*, 2009, **30**, 1482–1491.
6 M. T. Wolf, K. A. Daly, E. P. Brennan-Pierce, S. A. Johnson, C. A. Carruthers, A. D'Amore, S. P. Nagarkar, S. S. Velankar and S. F. Badylak, *Biomaterials*, 2012, **33**, 7028–7038.
7 T. Gilbert, T. Sellaro and S. Badylak, *Biomaterials*, 2006, **27**, 3675–3683.
8 J. Kort-Mascort, S. Flores-Torres, O. Peza-Chavez, J. H. Jang, L. A. Pardo, S. D. Tran and J. Kinsella, *Biomater. Sci.*, 2023, **11**, 400–431.
9 J. A. Owley, G. Madlambayan and D. J. Mooney, *Biomaterials*, 1999, **20**, 45–53.
10 J. Lou, R. Stowers, S. Nam, Y. Xia and O. Chaudhuri, *Biomaterials*, 2018, **154**, 213–222.

11 J. A. Burdick and K. S. Anseth, *Biomaterials*, 2002, **23**, 4315–4323.
12 A. Nishiguchi, S. Ito, K. Nagasaka, H. Komatsu, K. Uto and T. Taguchi, *Biomaterials*, 2024, **305**, 122451.
13 H. Komatsu, S. Watanabe, S. Ito, K. Nagasaka, A. Nishiguchi and T. Taguchi, *Macromol. Biosci.*, 2023, **23**, e2300097.
14 S. Ito, K. Nagasaka, H. Komatsu, D. Palai, A. Nishiguchi and T. Taguchi, *Biomater. Adv.*, 2024, **159**, 213834.
15 A. Nishiguchi, E. Araki, D. Palai, S. Ito and T. Taguchi, *Biomacromolecules*, 2024, **25**, 6146–6154.
16 A. Nishiguchi and T. Taguchi, *J. Mater. Chem. B*, 2023, **11**, 4005–4013.
17 D. Palai, M. Ohta, I. Cetnar, T. Taguchi and A. Nishiguchi, *Biomater. Sci.*, 2024, **12**, 2312–2320.
18 S. Ahadian, R. B. Sadeghian, S. Salehi, S. Ostrovidov, H. Bae, M. Ramalingam and A. Khademhosseini, *Bioconjugate Chem.*, 2015, **26**, 1984–2001.
19 N. Huebsch, P. R. Arany, A. S. Mao, D. Shvartsman, O. A. Ali, S. A. Bencherif, J. Rivera-Feliciano and D. J. Mooney, *Nat. Mater.*, 2010, **9**, 518–526.
20 D. E. Discher, P. Janmey and Y.-L. Wang, *Science*, 2005, **310**, 1139–1143.
21 A. J. Engler, S. Sen, H. L. Sweeney and D. E. Discher, *Cell*, 2006, **126**, 677–689.
22 O. Chaudhuri, S. T. Koshy, C. B. da Cunha, J.-W. Shin, C. S. Verbeke, K. H. Allison and D. J. Mooney, *Nat. Mater.*, 2014, **13**, 970–978.
23 D. D. McKinnon, D. W. Domaille, J. N. Cha and K. S. Anseth, *Adv. Mater.*, 2014, **26**, 865–872.
24 O. Chaudhuri, L. Gu, M. Darnell, D. Klumpers, S. A. Bencherif, J. C. Weaver, N. Huebsch and D. J. Mooney, *Nat. Commun.*, 2015, **6**, 6364.
25 A. J. Sutherland, G. L. Converse, R. A. Hopkins and M. S. Detamore, *Adv. Healthcare Mater.*, 2015, **4**, 29–39.
26 S. Lee, H. S. Lee, J. J. Chung, S. H. Kim, J. W. Park, K. Lee and Y. Jung, *Int. J. Mol. Sci.*, 2021, **22**, 2886.
27 A. Nishiguchi and T. Taguchi, *Acta Biomater.*, 2021, **131**, 211–221.
28 P. K. Parameshwar, L. Sagrillo-Fagundes, C. Fournier, S. Girard, C. Vaillancourt and C. Moraes, *Biomater. Sci.*, 2021, **9**, 7247–7256.
29 O. Chaudhuri, J. Cooper-White, P. A. Janmey, D. J. Mooney and V. B. Shenoy, *Nature*, 2020, **584**, 535–546.
30 A. Nishiguchi, H. Ichimaru, S. Ito, K. Nagasaka and T. Taguchi, *Acta Biomater.*, 2022, **146**, 80–93.
31 K. Sadtler, K. Estrellas, B. W. Allen, M. T. Wolf, H. Fan, A. J. Tam, C. H. Patel, B. S. Luber, H. Wang, K. R. Wagner, J. D. Powell, F. Housseau, D. M. Pardoll and J. H. Elisseeff, *Science*, 2016, **352**, 366–370.
32 E. M. Carvalho, E. A. Ding, A. Saha, D. C. Garcia, A. Weldy, P.-J. H. Zushin, A. Stahl, M. K. Aghi and S. Kumar, *Adv. Mater.*, 2024, **36**, e2404885.
33 O. Chaudhuri, *Biomater. Sci.*, 2017, **5**, 1480–1490.
34 M. Ahearne, Y. Yang, A. J. El Haj, K. Y. Then and K.-K. Liu, *J. R. Soc., Interface*, 2005, **2**, 455–463.
35 O. Chaudhuri, L. Gu, D. Klumpers, M. Darnell, S. A. Bencherif, J. C. Weaver, N. Huebsch, H.-P. Lee, E. Lippens, G. N. Duda and D. J. Mooney, *Nat. Mater.*, 2016, **15**, 326–334.
36 P. Ghosh, A. P. Rameshbabu and S. Dhara, *Langmuir*, 2014, **30**, 8442–8451.
37 S. Khetan, M. Guvendiren, W. R. Legant, D. M. Cohen, C. S. Chen and J. A. Burdick, *Nat. Mater.*, 2013, **12**, 458–465.